TECHNICAL REPORT 2089
September 2015

Simulated bi-SQUID Arrays Performing Direction Finding

Susan Berggren
Benjamin Taylor
Anna Leese de Escobar
SSC Pacific

Thomas Sheffield
Southern Methodist University

Daniel Hallman
California State University, Long Beach

SSC Pacific
San Diego, CA 92152-5001

SSC Pacific
San Diego, California 92152-5001

K. J. Rothenhaus, CAPT, USN
Commanding Officer

C. A. Keeney
Executive Director

ADMINISTRATIVE INFORMATION

The work described in this report was performed by the Advanced Concepts & Applied Research Branch (Code 71730), Space and Naval Warfare Systems Center Pacific (SSC Pacific), San Diego, CA. The Naval Innovative Science and Engineering (NISE) Program at SSC Pacific funded this Applied Research project.

Released by
K. Simonsen, Head
Advanced Concepts & Applied
Research Branch

Under authority of
A. Ramirez, Head
Advanced Systems and
Applied Sciences Division

SB

EXECUTIVE SUMMARY

OBJECTIVE

One of the High Temperature Superconductor (HTS) bi-Superconducting Quantum Interference Device (SQUID) Array Fractional Wavelength Baseline Determination and Design Study team's goal was to determine whether the raw simulated output from an array of bi-superconducting quantum interference devices (bi-SQUIDs) could perform direction-finding (DF) tasks such as the angle of arrival (AoA), elevation, and polarization. First, we applied the multiple signal classification (MUSIC) algorithm on linearly polarized signals. We included multiple signals in the output both of the same frequency and different frequencies. Next, we explored a modified MUSIC algorithm called dimensionality reduction MUSIC (DR-MUSIC), which can handle elliptical or circular polarizations. Finally, we explored the six-element Poynting vector method.

RESULTS

We determined that the MUSIC algorithm is able to determine the AoA from the simulated SQUID data for linearly polarized signals. The MUSIC algorithm could accurately find multiple signals of different frequency, and if there were $k + 1$ sensors, it could find k signals of the same frequency. Unfortunately, if signal polarizations are circular or elliptic, desired phase differences (due to the antenna separations) are changed by the signal polarizations and the MUSIC algorithm cannot find the direction-of-arrival (DoA) angles. We explored some modified algorithms, including DR-MUSIC, which performed well with both smaller baselines and signal polarizations.

The Poynting vector algorithm performed well for any polarization. The disadvantage of this method is that it requires electric field antenna measurements to capture all six components. As a result, the SQUID-based sensor size benefit is reduced and applications are restricted. Outside frequencies of interest, the Poynting vector error increased when the separation between arrays was the same magnitude as the signal wavelength.

RECOMMENDATIONS

We determined it is possible to apply DF when using bi-SQUID array sensors. Future tests should scale up the array used and determine the distance limits between arrays. We are also exploring other configurations that use both phase difference and Poynting vector algorithms for all DF tasks with any polarization without the need to use electric field sensors. Finally, experiments in this report were conducted using computer simulation of a bi-SQUID array sensor; we will need to verify all algorithms with experimental data.

CONTENTS

Figures

Tables

1. INTRODUCTION

Superconducting quantum interference devices (SQUIDs) are magnetometers that use macroscopic quantum effects to achieve unprecedented sensitivity to surrounding magnetic fields. A direct current (DC) SQUID has two Josephson junctions in a ring of superconducting material. Adding a third junction bisecting the superconducting loop increases the linearity of the voltage response output [1]. This device is called a DC bi-SQUID.

Through recent developments [2, 3], the idea of turning a SQUID (or bi-SQUID) or an array of SQUIDs (or bi-SQUIDs) into a working antenna is becoming a reality. One step to accomplishing this goal is to adopt or develop a method that would allow a SQUID (or bi-SQUID) array sensor to perform direction finding (DF) (i.e., locate the source of a signal). The simplest way to achieve this performance goal is to spatially separate multiple SQUID (or bi-SQUID) arrays to exploit natural phase differences induced by separations. Other methods involve distinctly polarized arrays that sense the Cartesian components of the electromagnetic waves.

In this report, we apply apply multiple signal classification (MUSIC) [4], dimensionality reduction MUSIC (DR-MUSIC) [5], and Poynting vector [6] algorithms to a small simulated array of bi-SQUID array sensors and record their performance against a variety of different arrival angles and polarizations. To maximize the utility that a bi-SQUID array may offer, the project team focused on small and linear arrays consisting of two to three antennas so that they are installed on different platforms. We are exploring other potential methods [7–11].

2. BACKGROUND: ARRAY SIMULATION

To simulate data that is fed into the DF algorithms, we use the schematic of the series coupled array of DC bi-SQUIDs in Figure 1 to derive a system of equations that model the Josephson junction phase differences. In the circuit, (i_b, $i_{1,k}$, $i_{2,k}$, $i_{3,k}$, $i_{4,k}$, $i_{5,k}$) represent the normalized currents, ($\varphi_{1,k}$, $\varphi_{2,k}$, $\varphi_{3,k}$)) are the phases across the Josephson junctions, ($L_{1a,k}$, $L_{1b,k}$, $L_{2a,k}$, $L_{2b,k}$, $L_{3a,k}$, $L_{3b,k}$) are the parameters related to the inductance values, and $k = 1, ..., N$, and x_e are the points in the array where the contributions from external field and input signals are included.

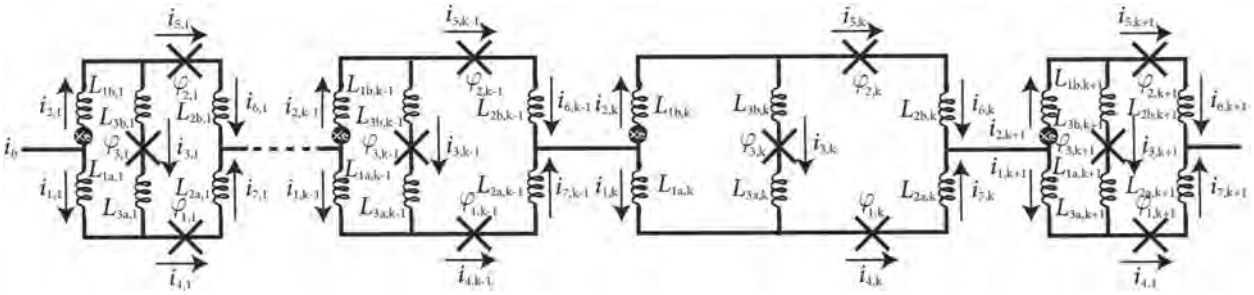

Figure 1. Schematic diagrams of a series coupled array of DC bi-SQUIDs.

To derive equations, we find current equations for the schematic diagram using Kirchhoff's current law and use the resistively shunted junction (RSJ) model of the over-damped Josephson junction with a lumped circuit representation. Both equations for bi-SQUID arrays and their derivations are found in [12, 13]. Some fabrication considerations are addressed in [14–16]. The system of equations is

$$
\begin{aligned}
&(L_{1,k}+L_{2a,k})\frac{d\varphi_{1,k}}{d\tau}-L_{2b,k}\frac{d\varphi_{2,k}}{d\tau}-L_{1,k}\frac{d\varphi_{3,k}}{d\tau}\\
&\quad=L_{1b,k}i_B+\varphi_{e,k}+\varphi_{2,k}-\varphi_{1,k}-(L_{1,k}+L_{2a,k})i_{c1,k}\sin\varphi_{1,k}+L_{1,k}i_{c3,k}\sin\varphi_{3,k}\\
&\qquad+L_{2b,k}i_{c2,k}\sin\varphi_{2,k}+\sum_{i\neq k}\frac{M}{d_i^3a_i}(\varphi_{1,i}-\varphi_{2,i}-2\pi x_e a_i)\\
&L_{2}a\frac{d\varphi_{1,k}}{d\tau}-(L_{1,k}+L_{2b,k})\frac{d\varphi_{2,k}}{d\tau}-L_{1,k}\frac{d\varphi_{3,k}}{d\tau}\\
&\quad=-L_{1a,k}i_B+\varphi_{e,k}+\varphi_{2,k}-\varphi_{1,k}+(L_{1,k}+L_{2b,k})i_{c2,k}\sin\varphi_{2,k}+L_{1,k}i_{c3,k}\sin\varphi_{3,k}\\
&\qquad-L_{2a,k}i_{c1,k}\sin\varphi_{1,k}+\sum_{i\neq k}\frac{M}{d_i^3a_i}(\varphi_{1,i}-\varphi_{2,i}-2\pi x_e a_i)\\
&L_{2a,k}\frac{d\varphi_{1,k}}{d\tau}-L_{2b,k}\frac{d\varphi_{2,k}}{d\tau}+L_{3,k}\frac{d\varphi_{3,k}}{d\tau}\\
&\quad=\varphi_{2,k}-\varphi_{1,k}-\varphi_{3,k}-L_{2a,k}i_{c1,k}\sin\varphi_{1,k}+L_{2b,k}i_{c2,k}\sin\varphi_{2,k}-L_{3,k}i_{c3,k}\sin\varphi_{3,k},
\end{aligned}
\tag{1}
$$

where $\varphi_{1,k}$, $\varphi_{2,k}$, and $\varphi_{3,k}$ are phases across the Josephson junction in each bi-SQUID, $k = 1, ..., N$, N is the number of bi-SQUIDs in the array, M is the coupling parameter, and $L_{1,k} = L_{1a,k} + L_{1b,k}$, $L_{3,k} = L_{3a,k} + L_{3b,k}$. Dots denote the time differentiation with normalized time $\tau = \omega_c t$, where t is time, $\omega_c = 2eI_0R_N/\hbar$, and the normalizing current of the Josephson junctions is I_0. The parameter R_N in ω_c is the normal state resistance of the Josephson junctions, e is the charge of an electron, and $\hbar$ is the reduced Planck constant. The parameter i_b is the normalized bias current and $\varphi_{e,k} = 2\pi x_e a_k$, where a_k is the normalized bi-SQUID area. We use the approximate assumption that $a_k = L_{1a,k}+L_{1b,k}+L_{2a,k}+L_{2b,k}$.

To model the array, the differential equations in Equation (1) are integrated in MATLAB® and the array voltage over time $V(t) = \sum_{i=1}^{N}\left(\frac{\dot\varphi_{1,k}+\dot\varphi_{2,k}}{2}\right)$ is plotted. See Figure 2 for an example of $V(t)$.

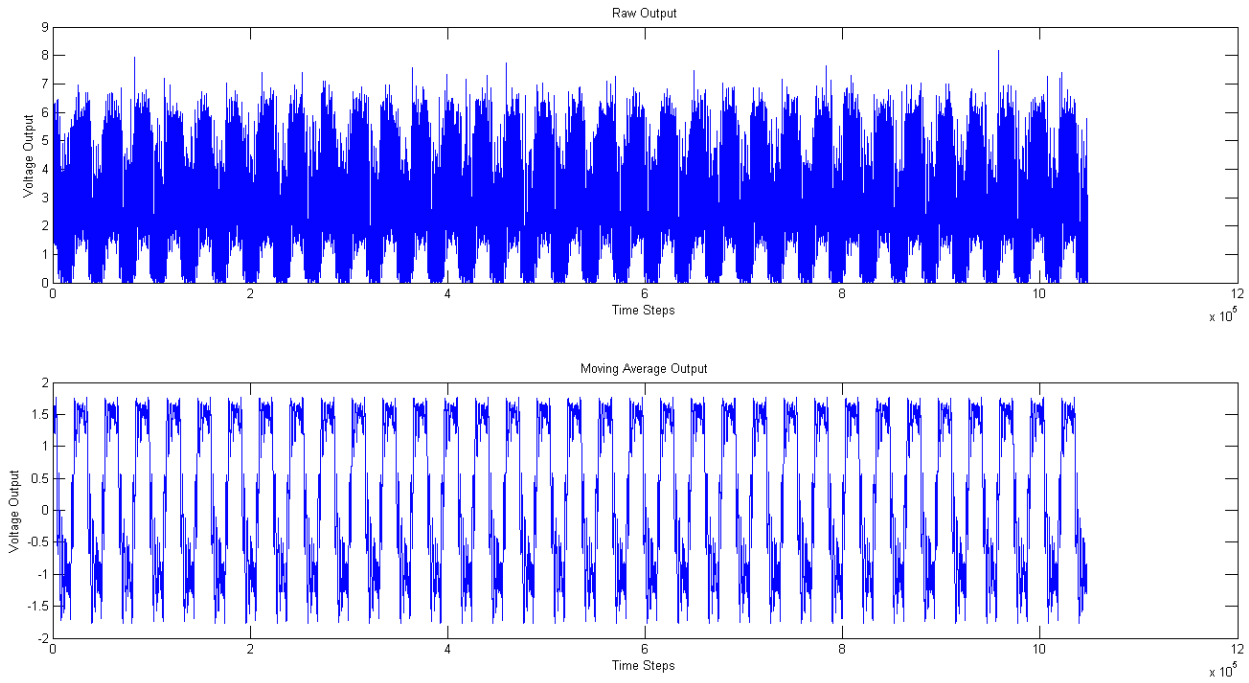

Figure 2. A bi-SQUID array $V(t)$ with multiple signals of different strengths and polarizations. The top plot is raw data and the bottom is the data after passing through a filter that removes the terahertz bi-SQUID response.

Multiple sensors are necessary for the feasibility of any DoA estimation. The bi-SQUID simulation program is only equipped to emulate a single bi-SQUID array sensor. To compensate, we assume that we have two or more identical bi-SQUID array sensors that are located at distances we select. Inputting a signal into the bi-SQUID program results in an estimate of the voltage response that a true bi-SQUID array would create in the presence of the signal. To replicate the output of additional sensors that were physically displaced, we input the same signal but doped with a predetermined phase difference that is specific to the AoA we elected to simulate.

For K signals $(\mathbf{s}_1(t), \ldots, \mathbf{s}_K(t))$ impinging on a uniform linear array, the signal received by the m^{th} antenna is given as

$$c_k \mathbf{s}_k(t) \exp\left(\frac{j2(m-1)\pi\Delta}{\lambda_k}\cos\phi_k\right), \tag{2}$$

where Δ is the length of separation between antennas (baseline), λ_k is the wavelength of the k^{th} signal, and $0 \leq \phi_k < 2\pi$ is the arrival azimuth of the k^{th} signal. The parameter c_k represents a complex scalar that is derived from the relationship between signal parameters and antenna polarizations. When a bi-SQUID array simulator does not accept a complex-valued input, Equation (2) is replaced with

$$z_k \mathbf{s}_k\left(t + \theta_k + \frac{j2(m-1)\pi\Delta}{\lambda_k}\cos\phi_k\right), \tag{3}$$

where $z_k = |c|$ and $\theta_k = \arg(c_k)$. We can replace Equation (2) with Equation (3) because the exponential and complex terms in Equation (2) represent phase differences that we can easily transfer into the real-valued signal itself. If our signal takes the form of Equation (3), a Hilbert transform is applied to the resulting output of the bi-SQUID array simulation. The Hilbert transform allows us to complete the analytic signal necessary for use in DF algorithms.

3. APPLYING THE MULTIPLE SIGNAL CLASSIFICATION ALGORITHM

The first algorithm we explore is the MUSIC algorithm [4] with a uniform linear array of bi-SQUID array sensors.

3.1 SUMMARY OF MUSIC

Integer K number of polarized narrowband electromagnetic waves traveling through the far field through a homogeneous isotropic medium impinge on an array consisting of integer L number of uniformly polarized antennas uniformly spaced at no more than a half-wavelength apart from each other. Data collected by L antennas are represented by

$$\begin{aligned} \mathbf{X}(t) &= \sum_{k=1}^{K} \mathbf{a}_k \mathbf{s}_k(t) + \mathbf{n}(t) \\ &= \mathbf{A}\mathbf{s}(t) + \mathbf{n}(t), \end{aligned} \tag{4}$$

where

$$\mathbf{a}(\phi_k) = \begin{bmatrix} 1 \\ e^{j\mu_k} \\ \vdots \\ e^{j(L-1)\mu_k} \end{bmatrix}$$

is the steering vector for the k^{th} signal, $\mathbf{n}(t)$ is the zero-mean additive complex Gaussian noise and $\mu_k = 2\pi\Delta\cos(\phi_k)/\lambda_k$. For the matrix notation, $\mathbf{A} = [\mathbf{a}_1, \ldots, \mathbf{a}_K]$. The data matrix $\mathbf{X}$ is an $L \times N$ matrix where N is the number of data samples recorded in a given interval of time.

The covariance matrix of the data $\mathbf{X}(t)$ is given by

$$\mathbf{R}_x = \mathrm{E}[\mathbf{X}\mathbf{X}^{\mathrm{H}}] = \mathbf{A}\mathbf{R}_s\mathbf{A}^{\mathrm{H}} + \sigma^2\mathbf{I},$$

where $(\cdot)^{\mathrm{H}}$ denotes complex conjugate transpose, σ^2 is the white noise power, and $\mathbf{R}_s = \mathrm{E}[\mathbf{s}^{\mathrm{H}}(t)\mathbf{s}(t)]$ is the source covariance matrix. We can easily estimate $\mathbf{R}_x$ with

$$\mathbf{R} = \frac{1}{N}\mathbf{X}\mathbf{X}^{\mathrm{H}}.$$

MUSIC begins by executing an eigendecomposition on the matrix $\mathbf{R}$. The resulting eigenvectors decompose the data correlation matrix into a K-dimensional signal subspace and an $(L-K)$-dimensional noise subspace. Let $\mathbf{E}_n$ represent the $L \times (L-K)$ matrix of noise eigenvectors associated with the $(L-K)$ smallest eigenvalues of $\mathbf{R}$. The MUSIC spectrum is then given as

$$\mathbf{P}_{\mathrm{MU}}(\theta_k, \phi_k) = \left[\frac{\mathbf{a}^H(\phi_k)\mathbf{E}_n\mathbf{E}_n^H\mathbf{a}(\phi_k)}{\mathbf{a}^H(\phi_k)\mathbf{a}^H(\phi_k)}\right]^{-1}.$$

The peaks of this spectrum will correspond to the desired azimuth angles to be found (Figure 3). The left plot is the raw $V(t)$ data with two signals of 300 MHz and 3 GHz. The right plot is the AoA for the 300-MHz signal as determined by the MUSIC algorithm.

For a distinctly polarized or uniform rectangular array of antennas, the corresponding steering vector $\mathbf{a}(\theta_k, \phi_k)$ allows MUSIC to perform a two-dimensional (2-D) search so that elevation can be found in addition to the azimuth. In the case where only azimuth is considered, elevation is held constant at $\pi/2$ radians.

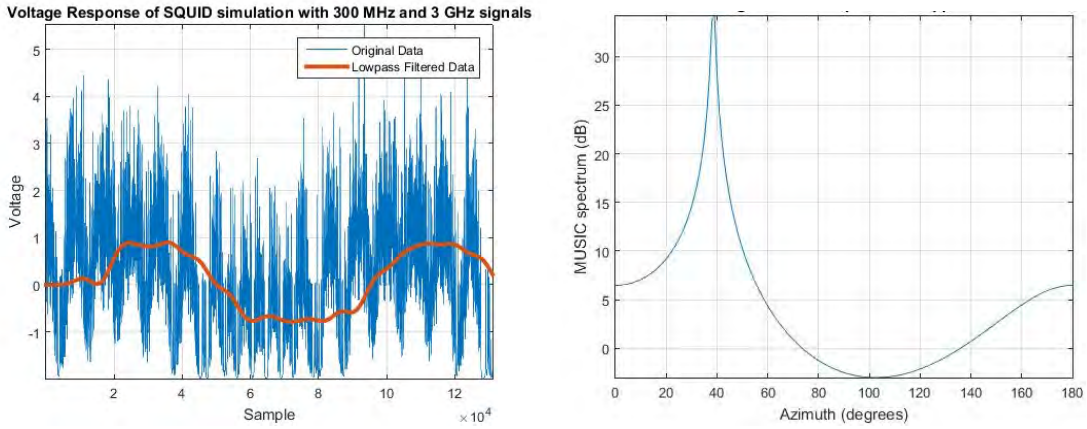

Figure 3. Left: bi-SQUID array $V(t)$ with two signals of 300 MHz and 3 GHz. Right: the AoA for the 300-MHz signal as determined by the MUSIC algorithm.

3.2 MULTIPLE SIGNALS, DIFFERENT FREQUENCIES

For conventional antenna arrays with a limited bandwidth, there are a limited number of frequencies detected. In contrast to the limited bandwidth of a conventional antenna, the bandwidth of a bi-SQUID array sensors is extended, which leads to an increase in active signals. To compensate for these increases, two to three bi-SQUID array sensors coupled with digital filters are used to maintain their extremely small profile while preserving acceptable performance in the presence of many impinging signals of differing frequencies. Digital filters offer the ability to block unwanted frequency ranges so that MUSIC can find the DoA angles selectively.

For the first experiment (Table 1), we test the MUSIC algorithm against a bi-SQUID array simulation of two uniformly polarized sensors that have received one signal. We test limits by steadily decreasing the baseline until failure. The baselines listed are in units of wavelengths. Each test used 2^{17} data samples.

Table 1. Azimuth estimate using MUSIC.

Baseline	ϕ	ϕ_{est}	Error
1/2	145	145	0
1/2	10	9	1
1/10	45	46	1
1/10	120	119	1
1/25	10	20	10
1/25	80	80	0
1/25	165	156	9
1/50	30	46	16
1/50	30	122	92

For the second experiment, we introduce one 3-GHz signal and one 300-MHz signal into the simulation and try to find the angles with MUSIC. This experiment is for three uniformly spaced identical bi-SQUID array sensors. While searching for both signals, it is possible to tune the steering vector (i.e., change the phase difference to match a particular wavelength) in our search to focus on one signal at a time. In place of this approach, we use filters to block the unwanted signal and tell MUSIC that only one signal is present. This approach yields better results (Table 2). Two baselines listed in each row correspond to the 3-GHz and 300-MHz signals, respectively.

Table 2. Two signals found separately using filters.

Baseline	ϕ_1	ϕ_2	$\phi_{1\ \mathrm{est}}$	$\phi_{2\ \mathrm{est}}$	Error
1/2, 1/20	15	135	15	135	0, 0
	20	60	20	60	0, 0
1/5, 1/50	20	150	19	161	1, 11
	45	90	46	91	1, 1
1/10, 1/100	110	160	110	180	0, 20
	20	55	23	87	3, 64

3.3 MULTIPLE SIGNALS, SINGLE FREQUENCY

The MUSIC algorithm has the option of finding multiple signals of the same frequency simultaneously, in addition to its accuracy and easy implementation. However, in the presence of k signals, MUSIC requires $k + 1$ antennas for reliable DF. Hence, for an array with three elements, a maximum of only two signals with the same carrier frequency can be located. For situations where this constraint is too restrictive, an array with more sensors is preferred. Table 3 show results from simulations with two incoherent signals impinging on a three-element uniformly polarized array with identical carrier frequencies. The MUSIC algorithms' ability to find signals simultaneously is used to find the angles since is not possible to focus on one signal at a time.

Table 3. Two signals found simultaneously.

Baseline	ϕ_1	ϕ_2	$\phi_{1\ \mathrm{est}}$	$\phi_{2\ \mathrm{est}}$	Error
1/2	110	160	109	158	1, 2
	40	140	35	134	5, 6
	15	115	8	114	7, 1
1/10	80	110	81	113	1, 3
	90	100	90	99	0, 1
1/25	10	170	35	35	25, 135
	45	135	59	59	14, 76

3.4 POLARIZED SIGNALS

Unfortunately, if signal polarizations are circular or elliptic, the desired phase differences invoked by the antenna separations are polluted by the independent phases that result from the interactions of the polarization and the signal phase differences. The MUSIC algorithm inconsistently finds DoA angles in this situation unless a modified technique is used [5, 9, 11]. While using an ordinary form of the MUSIC algorithm, we restrict our signals exclusively to linear polarization.

4. DIMENSIONALITY REDUCTION MULTIPLE SIGNAL CLASSIFICATION

While the previous section was useful for signals with linear polarizations, they do not perform well with elliptical or circular polarizations. To achieve accuracy when working with signals possessing varied polarizational phase differences, we can use a technique called DR-MUSIC [5]. The DR-MUSIC algorithm is designed to work with a six-element colocated vector sensor. The components of the electromagnetic wave of an incoming signal is picked up by the vector sensor and is expressed as

$$\mathbf{a}_k(\theta_k, \phi_k, \gamma_k, \eta_k) = \begin{bmatrix} e_{kx} \\ e_{ky} \\ e_{kz} \\ h_{kx} \\ h_{ky} \\ h_{kz} \end{bmatrix} = \begin{bmatrix} \cos\theta_k \cos\phi_k & -\sin\phi_k \\ \cos\theta_k \sin\phi_k & cos\phi_k \\ -\sin\theta_k & 0 \\ -\sin\phi_k & -\cos\theta_k \cos\phi_k \\ \cos\phi_k & -\cos\theta_k \sin\phi_k \\ 0 & \sin\theta_k \end{bmatrix} \begin{bmatrix} \sin\gamma_k e^{j\eta_k} \\ \cos\gamma_k \end{bmatrix}, \tag{5}$$

where $-\pi \leq \eta_k \leq \pi$ is the polarization phase difference of the k^{th} signal. Denote the larger matrix of Equation (5) as $\mathbf{\Omega}(\theta_k, \phi_k)$. The matrix of data $\mathbf{X}$ is found in the same way as in Equation (4) but with new steering vectors shown in Equation (5). Eigendecomposition is performed on the data correlation matrix and we now let $\mathbf{U}_n$ represent the noise eigenvectors of the data. We define a new matrix:

$$\mathbf{B}(\theta_k, \phi_k) \triangleq \mathbf{\Omega}^{\text{H}} \mathbf{U}_n \mathbf{U}_n^{\text{H}} \mathbf{\Omega}.$$

The DR-MUSIC algorithm states that the minimum eigenvalue of $\mathbf{B}$ is smallest precisely when $\mathbf{B}$ is evaluated at the correct DoAl angles. Thus, the DR-MUSIC spatial spectrum is

$$\mathbf{P}_{\text{DR}}(\theta_k, \phi_k) = \left[\min_{\theta_k, \phi_k} \lambda_{\text{min}}(\mathbf{B}(\theta_k, \phi_k)) \right]^{-1}.$$

Table 4 uses the modified version of DR-MUSIC to find the arrival angles of one signal impinging on three orthogonally oriented non-colocated bi-SQUID array sensors. The signal is allowed to have circular or elliptical polarizations; therefore, parameters are varied with each trial.

Table 4. Non-colocated DR-MUSIC.

Baseline	γ	η	ϕ	θ	ϕ_{est}	θ_{est}	Error
1/2	$\pi/3$	0	145	45	144	45	1, 0
	$\pi/6$	-$\pi/4$	170	25	170	25	0, 0
1/10	$\pi/6$	-$\pi/4$	170	2	170	4	0, 2
	1	-1	90	5	93	3.5	3, 1.5
1/25	$2\pi/5$	$\pi/6$	10	90	9	90	1, 0
	$2\pi/5$	$\pi/6$	100	5	108	3.5	8, 1.5
1/50	$\pi/6$	-$\pi/4$	170	25	169	24.5	1, 0.5
	$2\pi/5$	$\pi/6$	100	5	106	3	6, 2
1/100	$\pi/2.5$	-$3\pi/4$	10	20	8	18	2, 2
	$\pi/5$	$\pi/4$	12	87	12	86.5	0, 0.5
1/500	$\pi/5$	$\pi/3$	80	80	80	79	0, 1
	$\pi/3$	$\pi/2$	145	45	146	45	1, 0

5. POYNTING VECTOR

We explored alternate ways to achieve the AoA, elevation, and polarization information [6–8, 10]. In this section, we explore the Poynting vector method.

5.1 SUMMARY OF THE POYNTING VECTOR

The Poynting vector method is the most robust way to match a small baseline bi-SQUID array arrangement with relatively long wavelengths. The computations and processing are simple and the error lowers at longer wavelengths. One disadvantage is that a tripole antenna is needed to measure electric fields; therefore, you lose the advantage of using bi-SQUID arrays. This method would also need to distinguish multiple signals and handle multipath signals. The Poynting vector method takes the voltage output from each sensor to get the field component in that direction. Then, a cross product is taken to find the Poynting vector k (Figure 4).

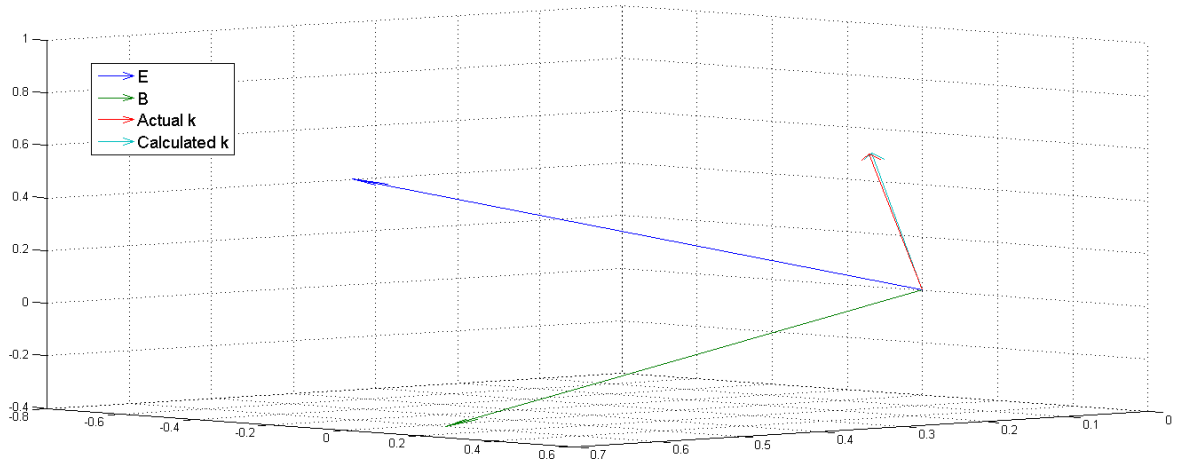

Figure 4. Sample calculation of the Poynting vector from bi-SQUID array data.

The direction of the source is simply the negative of the cross product:

$$\mathbf{k} = \mathbf{E} \times \mathbf{B}.$$

One can also do 2-D DF with only three sensors: (B_x, B_y, E_z). However, this only works with vertically polarized sources, that is, when $B_z = 0$. The expressions $k_x = -B_y E_z$ and $k_y = E_z B_x$ are used to find the x and y components of the Poynting vector.

Three separate bi-SQUID array simulations are used to generate magnetic field vector sensor data, each with a specific input flux and phase difference due to separation. A simple model of electric fields with some noise is added to compute the Poynting vector and to give the angle error and vector quiver plots. The elevation and azimuth of the Poynting vector is the direction the signal is traveling, which is the negative of the vector pointing toward the source.

Equations for both the x and y components of the magnetic field inside of a polarization ellipse perpendicular to the Poynting vector when pointing in the z direction is

$$\mathbf{B} = |\mathbf{B}| \begin{bmatrix} \cos\theta_B \cos(\omega t) \\ \sin\theta_B \cos(\omega t + \alpha_y) \\ 0 \end{bmatrix}.$$

Here, ω is the angular frequency, θ_B is the angle between $\mathbf{B}$ and the x-axis, and α_y is the polarization phase difference. By rotating the whole system around the y-axis by the elevation angle φ_k and then rotating that around the z-axis by the azimuthal angle θ_k, we get the full equation for the magnetic field at the center of the cube:

$$\mathbf{B} = |\mathbf{B}| \begin{bmatrix} \cos\theta_k \cos\varphi_k \cos\theta_B \cos(\omega t) - \sin\theta_k \sin\theta_B \cos(\omega t + \alpha_y) \\ \sin\theta_k \cos\varphi_k \cos\theta_B \cos(\omega t) + \cos\theta_k \sin\theta_B \cos(\omega t + \alpha_y) \\ -\sin\varphi_k \cos\theta_B \cos(\omega t) \end{bmatrix}.$$

The flux received by each sensor should correspond with the component of this vector. Parameter $\bar{t}$ represents the time shift a signal will undergo based on the distance between a given detector and the center of the cube:

$$\bar{t} = t - \frac{\vec{s} \cdot \hat{k}}{c},$$

where $\vec{s}$ is the position vector pointing from the cube center to the sensor, c is the speed of light, and $\hat{k}$ is the normalized Poynting vector. Since each sensor is shifted from the center in the same direction it points, the x component of k is used for the x sensor (in spherical coordinates). Lastly, a moving average is used to clean up remove the higher frequencies in the output and shift the data vertically so that it's approximately oscillating around zero.

To simulate the electric field, equations for the $\mathbf{B}$ field were clockwise by 90 degrees in the polarization ellipse, so that

$$\mathbf{E} = \begin{bmatrix} \cos\theta_k \cos\varphi_k \sin\theta_B \cos(\omega t + \alpha_y) + \sin\theta_k \cos\theta_B \cos(\omega t + \alpha_y) \\ \sin\theta_k \cos\varphi_k \sin\theta_B \cos(\omega t + \alpha_y) - \cos\theta_k \cos\theta_B \cos(\omega t) \\ -\sin\varphi_k \sin\theta_B \cos(\omega t + \alpha_y) \end{bmatrix}. \tag{6}$$

Figure 5 generates Equation (6). To reduce error, the $\mathbf{k}$ values when one of the $\mathbf{E}$ or $\mathbf{B}$ vectors are small are removed before taking a simple average.

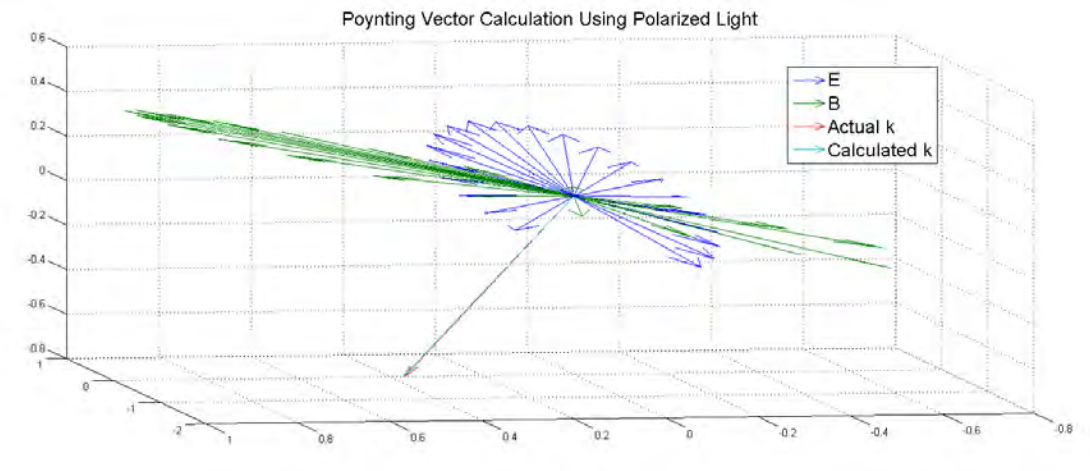

Figure 5. Both electric and magnetic fields rotating within the polarization ellipse.

5.2 SIMULATIONS

Direction of arrivals from the Poynting vector method are very accurate; they have less than a degree of error overall, which improves with longer detection time. The Poynting vector method also exhibits

good accuracy for varying frequency and polarization. Figure 6 shows the error in the Poynting vector for a linearly polarized source. The simulation length was set as three wavelengths long and the elevation was fixed to 45 degrees. Each sensor was separated from the center by one half of a centimeter while the highest frequency of 3 GHz corresponds to a wavelength of 10 cm. Ideally, each of these three sensors would colocate, but the separation only has a significant effect on accuracy when it has the same order as the wavelength or shorter.

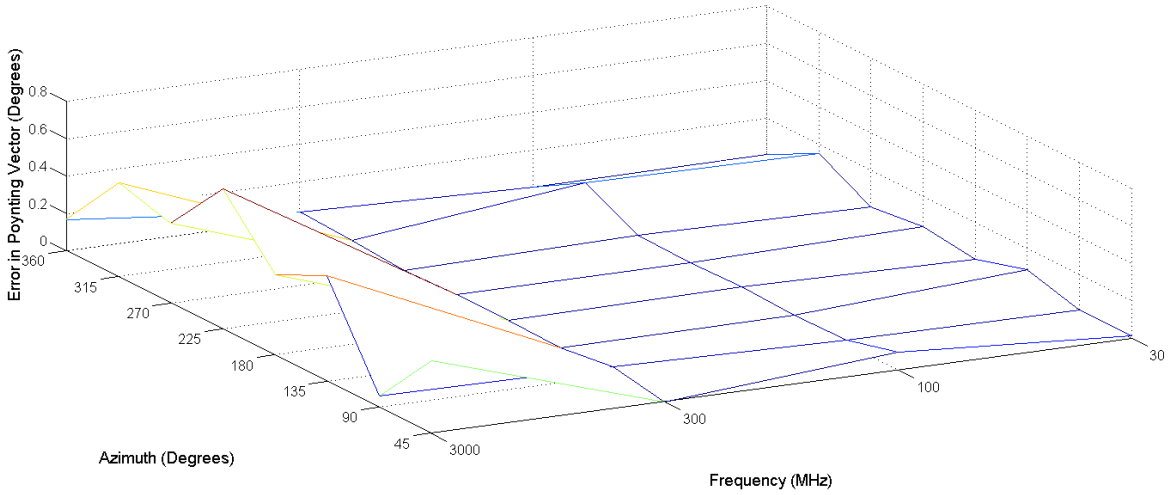

Figure 6. SQUID Poynting vector DF for a linearly polarized source.

Using the same simulation setup but a circularly polarized source, yields the results plotted in Figure 7. The circularly polarized light case gives a greater error, but this effect is small for longer wavelengths.

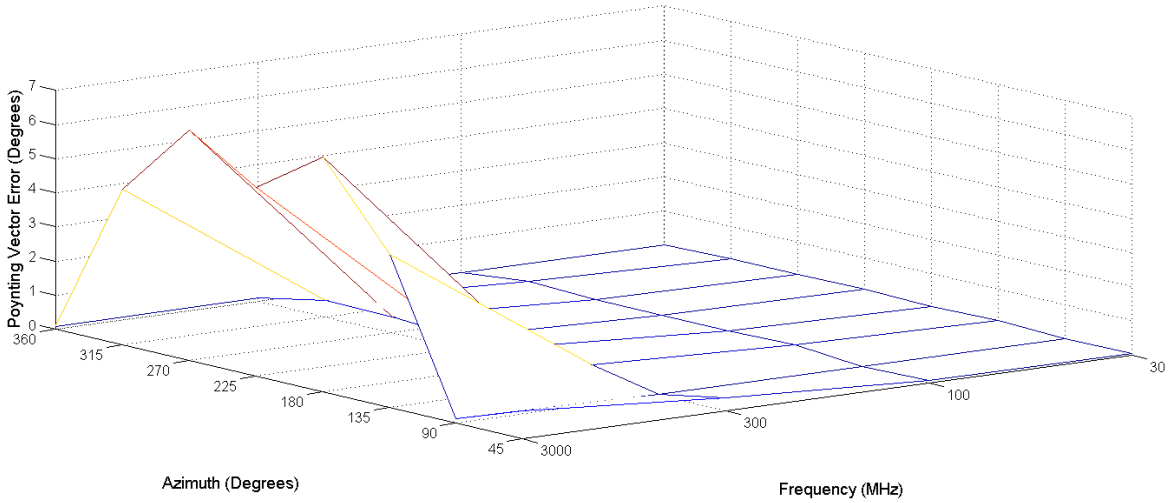

Figure 7. SQUID Poynting vector DF for a circularly polarized source.

6. CONCLUSION

This technical report offers an introduction into the outcomes of applying DF algorithms to data obtained from an array of bi-SQUID array sensors. We showed that it is possible to perform DF tasks with bi-SQUID arrays, though it is reasonable to assume the accuracy of the DF algorithms with a true bi-SQUID array will vary to some degree. Techniques presented here focus on a design that is as small as possible to maximize the number of applications for which the device can be used.

We determined that the MUSIC algorithm is a flexible subspace method that can perform in various situations. In addition, MUSIC can perform DF with multiple signals of the same frequency; however, MUSIC requires $k + 1$ sensors for k signals. If signal polarizations are circular or elliptic, MUSIC cannot reliably find the DoA angles. The DR-MUSIC algorithm can determine the DoA of signals featuring varied polarization from the bi-SQUID array simulated $V(t)$. The DR-MUSIC algorithm performed better with smaller baselines than the MUSIC algorithm.

Excellent polarization results occur when a cube of perpendicular bi-SQUID arrays paired with a tri-directional electric field antenna using the Poynting vector. To ignore the separation between sensors, the wavelength must be longer than a certain length, which is outside the wavelengths we are exploring in this study. Electrical field antennas may restrict the usage of the DF device due to their size.

Since bi-SQUID arrays can have multiple arrays on a single chip, the projects team's goal is to determine the possibility of performing an accurate DF when arrays differ in location by a matter of microns. Future improvements and signal processing techniques will be implemented to boost the accuracy and utility of these techniques for bi-SQUID array sensors. In this report, we conduct computer simulations of bi-SQUID array sensors in lieu of a real array data. Future work will apply existing DF methods to experimental data taken from a system of SQUID (or bi-SQUID) arrays.

REFERENCES

1. V. K. Kornev, I. I. Soloviev, N. V. Klenov, and O. A. Mukhanov. 2009. "Bi-SQUID: A Novel Linearization Method for DC SQUID Voltage Response," *Superconductor Science and Technology 22*:114011.

2. M. C. de Andrade, B. Taylor, A. Leese de Escobar, S. Berggren, S. Dinh, R. Fagaly, J. Talvacchio, J. Przybysz, and B. Nechay. In Print. "Detection of Far Field Radio Frequency Signals by Niobium Superconducting Quantum Interference Device Arrays," *IEEE Transactions on Applied Superconductivity*.

3. G. Prokopenko, O. Mukhanov, and R. Romanofsky. In Print. "SQIF Antenna Measurement in Near Field," *2015 IEEE 15th International Superconductive Electronics Conference (ISEC)*.

4. Z. Chen, G. Gokeda, and Y. Yu. 2010. *Introduction to Direction-of-Arrival Estimation*. Artech House, Norwood, MA.

5. L. Wang, L. Yang, G. Wang, Z. Chen, and M. Zou. 2014. "Uni-Vector-Sensor Dimensionality Reduction MUSIC Algorithm for DoA and Polarization Estimation," *Mathematical Problems in Engineering 2014*:682472.

6. K. T. Wong and X. Yuan. 2011. "Vector Cross-Product Direction-Finding with an Electromagnetic Vector-Sensor of Six Orthogonally Oriented but Spatially Non-Collocating Dipoles/Loops," *IEEE Transactions on Signal Processing 59*:60–171.

7. K. T. Wong and M. D. Zoltowski. 1997. "Uni-Vector-Sensor ESPRIT for Multisource Azimuth, Elevation, and Polarization Estimation," *IEEE Transactions on Antennas and Propagation 45*:1467–1474.

8. E. R. Ferrara, and T. M. Parks. 1983. "Direction Finding with an Array of Antenna Having Diverse Polarizations," *IEEE Transactions on Antennas and Propagation AP-31*:231–236.

9. J. J. Whelan. 2010. "Diverse Polarization Extension to MUSIC Applied to a Circular Array of H-Plane Horns." Master's thesis. University of Dayton, Dayton, OH.

10. K. T. Wong and M. D. Zoltowski. 2000. "Closed-Form Direction-Finding with Arbitrarily Spaced Electromagnetic Vector-Sensors at Unknown Locations," *IEEE Transactions on Antennas and Propagation 48*:671–681.

11. K. T. Wong, L. Li, and M. D. Zoltowski. 2004. "Root-MUSIC-Based Direction-Finding and Polarization-Estimation Using Diversely-Polarized Possibly-Collocated Antennas," *IEEE Antennas and Wireless Propagation Letters 3*:129–132.

12. S. Berggren. 2012. "Computational and Mathematical Modeling of Coupled Superconducting Quantum Interference Devices." Doctoral dissertation. San Diego State University, San Diego, CA, and Claremont Graduate University, Claremont, CA.

13. P. Longhini, S. Berggren, A. Leese de Escobar, A. Palacios, S. Rice, B. Taylor, V. In., O. A. Mukhanov, G. Prokopenko, M. Nisenoff, E. Wong, and M. De Andrade. 2012. "Voltage Response of Non-Uniform Arrays of bi-Superconductive Quantum Interference Devices," *Journal of Applied Physics 111*:093920.

14. S. Berggren and A. Leese de Escobar. 2015. “Effects of Spread in Critical Currents for Series- and Parallel-Coupled Arrays of SQUIDs and Bi-SQUIDs.” *IEEE Transactions on Applied Superconductivity 25*:1600304.

15. S. M. Wu, S. A. Cybart, S. M. Anton, and R. C. Dynes. 2013. “Simulation of Series Arrays of Superconducting Quantum Interference Devices,” *IEEE Transactions on Applied Superconductivity 23*:1600104.

16. S. A. Cybart, T. N. Dalichaouch, S. M. Wu, S. M. Anton, J. A. Drisko, J. M. Parker, B. D. Harteneck, and R. C. Dynes. 2012. “Comparison of Measurements and Simulations of Series-parallel Incommensurate Area Superconducting Quantum Interference Device Arrays Fabricated from $YBa_2Cu_3O_{7-\delta}$ Ion Damage Josephson Junctions,” *Journal of Applied Physics 112*:063911.

REPORT DOCUMENTATION PAGE

Form Approved
OMB No. 0704-01-0188

PLEASE DO NOT RETURN YOUR FORM TO THE ABOVE ADDRESS.

1. REPORT DATE *(DD-MM-YYYY)*	**2. REPORT TYPE**	**3. DATES COVERED** *(From - To)*
September 2015	Final	

4. TITLE AND SUBTITLE

Simulated bi-SQUID Arrays Performing Direction Finding

5a. CONTRACT NUMBER

5b. GRANT NUMBER

5c. PROGRAM ELEMENT NUMBER

6. AUTHORS

Susan Berggren
Benjamin Taylor
Anna Leese de Escobar
SSC Pacific

Thomas Sheffield
Southern Methodist University

Daniel Hallman
California State University, Long Beach

5d. PROJECT NUMBER

5e. TASK NUMBER

5f. WORK UNIT NUMBER

7. PERFORMING ORGANIZATION NAME(S) AND ADDRESS(ES)

SSC Pacific, 53560 Hull Street, San Diego, CA 92152–5001

8. PERFORMING ORGANIZATION REPORT NUMBER

TR 2089

9. SPONSORING/MONITORING AGENCY NAME(S) AND ADDRESS(ES)

Naval Innovative Science and Engineering (NISE) Program (Applied Research)
SSC Pacific, 53560 Hull Street, San Diego, CA 92152–5001

10. SPONSOR/MONITOR'S ACRONYM(S)

11. SPONSOR/MONITOR'S REPORT NUMBER(S)

12. DISTRIBUTION/AVAILABILITY STATEMENT

Approved for public release.

13. SUPPLEMENTARY NOTES

14. ABSTRACT

One of the High-Temperature Superconductor (HTS) bi-Superconducting Quantum Interference Device (SQUID) Array Fractional Wavelength Baseline Determination and Design Study team's goal was to determine whether the raw simulated output from an array of bi-superconducting quantum interference devices (bi-SQUIDs) could perform direction-finding (DF) tasks, including the the angle of arrival (AOA), elevation, and polarization. First, we applied the multiple signal classification (MUSIC) algorithm on linearly polarized signals. We included multiple signals in the output both of the same frequency and different frequencies. Next, we explored a modified MUSIC algorithm called dimensionality reduction MUSIC (DR-MUSIC), which can handle elliptical or circular polarizations. Finally, we explored the six-element Poynting vector method.

15. SUBJECT TERMS

Mission Area: bi-Superconducting Quantum Interference Device (SQUID)

angle of arrival (AOA)	polarized signals	direction of arrival (DOA)
Poynting vector method	multiple signal classification (MUSIC)	dimensionality reduction MUSIC (DR-MUSIC)

16. SECURITY CLASSIFICATION OF:			**17. LIMITATION OF ABSTRACT**	**18. NUMBER OF PAGES**	**19a. NAME OF RESPONSIBLE PERSON**
a. REPORT	**b. ABSTRACT**	**c. THIS PAGE**			Susan Berggren
U	U	U	U	20	**19B. TELEPHONE NUMBER** *(Include area code)* (619) 553-2063

INITIAL DISTRIBUTION

84300	Library	(2)
85300	Archive/Stock	(1)
71730	S. Berggren	(3)
71730	B. J. Taylor	(1)
71730	A. Leese de Escobar	(1)

Defense Technical Information Center
Fort Belvoir, VA 22060–6218 (1)

Approved for public release.

SSC Pacific
San Diego, CA 92152-5001